Journal of Nuclear Materials 478 (2016) 74–82

Contents lists available at ScienceDirect

Journal of Nuclear Materials

journal homepage: www.elsevier.com/locate/jnucmat

# Concentration of constitutional and thermal defects in $UAl_4$

P.H. Gargano [a, b], L. Kniznik [a, b], P.R. Alonso [a, b], M.D. Forti [a, b], G.H. Rubiolo [a, b, c, *]

[a] Gerencia Materiales, Comisión Nacional de Energía Atómica, Av. Gral. Paz 1499, 1650, San Martín, Buenos Aires, Argentina
[b] Instituto de Tecnología J. Sabato, CNEA - UNSAM, Av. Gral. Paz 1499, 1650, San Martín, Buenos Aires, Argentina
[c] CONICET, Av. Rivadavia 1917, 1033, CABA, Argentina

## HIGHLIGHTS

- Formation energies of eight point defects in the four sublattices were calculated.
- Point defect concentrations were calculated as function of temperature and stoichiometry.
- The aluminum antisite is the constitutional point defect on the Al-rich side.
- On the Al-rich side, the dominant thermal defect is an interbranch defect.
- On the Al-rich side, Al atoms probably diffuse by the antisite bridge mechanism.

## ARTICLE INFO

*Article history:*
Received 19 January 2016
Received in revised form
2 May 2016
Accepted 30 May 2016
Available online 1 June 2016

*Keywords:*
Actinide materials and compounds
Point defects
Thermodynamic properties
DFT calculations

## ABSTRACT

The point defect structure of intermetallic compound oI20 $UAl_4$ is investigated using a combination of the statistical mechanical Wagner–Schottky model and first-principles calculations within a projector augmented wave pseudopotential method in conjunction with the generalized gradient approximation. The formation energies of eight point defects were calculated taking into account the four sublattices. The point defect concentrations are calculated as function of temperature and deviation from stoichiometry. Our results show that the aluminum antisite is the constitutional point defect on the Al-rich side. At this off-stoichiometric side the dominant thermal defect is an interbranch defect where four constitutional antisite aluminum atoms are replaced by five uranium vacancies. The point defect effective formation energies are obtained and these results allow us to identify the antistructure bridge mechanism as the most probable for the diffusion for Al atoms in the Al-rich $UAl_4$ intermetallic compound.


## 1. Introduction

Fuel cores for nuclear research and test reactors are aluminum matrix composites constituted of uranium alloys such as $UAl_x$ (mainly $UAl_3$) or $U_3Si_2$ dispersed in aluminum powder [1,2]. γ-U(Mo) alloys are now considered as the most promising candidates for the fuel core conversion of those research and test reactors currently using highly-enriched uranium (HEU) to low-enriched uranium (LEU) [3,4]. Therefore, reactions between U alloys and Al alloys are of great technical interest. The U-Al binary system has been extensively studied; it comprises three intermetallic compounds, viz. $UAl_2$, $UAl_3$, and $UAl_4$ ([5] and references therein).

In a previous work [6] we have satisfactorily simulated the growth of $UAl_4$ phase in an $UAl_3$/Al diffusion couple. We built a thermodynamic database using data from the literature and a kinetic database by adjusting parameters from reported experimental growth of the $UAl_4$ phase at different temperatures. Thermodynamic and kinetic databases were constructed that could be read with ThermoCalc [7] and DICTRA [8] packages. The $UAl_4$ compound was treated as a phase with solubility and assessed with a two-sublattice model where one sublattice is occupied by the Al atoms and the other by U atoms and Al antisites, no vacancies were considered. However, there is a controversy concerning the structure of point defects in the $UAl_4$ compound. To further improve our simulation, we have decided to clear this matter up.

Borie [9] has determined the crystallography of $UAl_4$ as body-centered orthorhombic, space group I2ma or Imma, from the analysis of X-ray diffraction patterns (XRD) and he obtained composition values in this phase between 81.8 and 83.1 at.% Al by chemical analysis. He also reported a density value for the

* Corresponding author. Gerencia Materiales, Comisión Nacional de Energía Atómica Av. Gral. Paz 1499, B1650KNA, San Martin, Buenos Aires, Argentina.
*E-mail address:* rubiolo@cnea.gov.ar (G.H. Rubiolo).

http://dx.doi.org/10.1016/j.jnucmat.2016.05.040
0022-3115/

compound of (5.7 ± 0.3) g/cm$^3$, while a perfect crystal should give a value of 6.1 g/cm$^3$. On this basis he postulated the existence of constitutional defects, U vacancies or Al substitutionals at U sites.

Some years later, Runnalls and Boucher [10] extended the research on the defect structure of the compound. They measured a density of (5.6 ± 0.1) g/cm$^3$. This low value was explained by the argument that some uranium sites are unoccupied. They also pointed out the occurrence of a transformation by nucleation and growth mechanism at 646 °C from their thermal analysis. It was attributed to a rearrangement or clustering of vacancies, transforming the high temperature β phase where the vacancies are randomly distributed into the $\alpha$ phase. The authors commented that little or no shift in uranium atom positions accompanied the transformation, but a movement of vacancies from aluminum to uranium sites could occur, since diffraction method was insensitive to aluminum positions.

Afterwards, Zenou et al. [11] analyzed powder XRD data of a $UAl_4$ sample with Rietveld refinement finding a good agreement when U occupancy is 90%, the amount of U vacancies was also confirmed by standard energy dispersive spectroscopy (81.5 ± 0.5 at % Al) and density (5.6 g/cm$^3$) measurements. However, Tougait and Noël [12] reported a similar work with the conclusion that the compound has a fully stoichiometric formation.

$UAl_4$ is finally assessed as an aluminum enriched compound with a homogeneity range between 80 and 82.8 at% Al which forms by a peritectic reaction between $UAl_3$ and liquid Al at 732 °C and a composition of 81.8 at% Al [13], and orthorhombic D1b structure (oI20, space group 74) exhibiting a polymorphic transformation Uβ ↔ U$\alpha$ at 646 °C [14].

To our best knowledge neither experimental nor theoretical investigations of the point defects energies and concentrations have been performed in the $UAl_4$ compound. We have recently reported [15] a thorough first principles study of $UAl_4$ atomic, electronic and magnetic configuration, together with an analysis of U and Al vacancies and antisites stability and electronic rearrangement taking into account the three possible aluminum sites according to Imma space group. In this paper, we use those results to estimate the energy of formation of point defects in the $UAl_4$ compound which we afterwards insert in a statistical thermodynamics formalism within the canonical ensemble [16,17] to predict equilibrium defect concentrations as a function of the alloy composition and temperature. As it will be shown, our calculations provide unambiguous support for the experimental results concerning the type of structural defects in the $UAl_4$ compound.

## 2. Method

In the following, we shall consider the $UAl_4$ ordered alloy which consists of four sublattices ($U;Al1;Al2;Al3$) corresponding to the lattice sites defined for the oI20 $UAl_4$ structure. Interstitials are not usually considered in studies of point defects in intermetallics, although some antecedents exist in the literature. The importance of self-interstitials in the equilibrium concentration of point defects has been detected recently in compounds with structures $D5_{19}$ ($Ni_2Al_3$) [18,19], $D8_8$ ($Si_3Ti_5$) [20] and $D0_{11}$ ($NiAl_3$) [21]. In a subsequent section of this work we discussed the critical errors in the modelling of the $UAl_4$ phase thermodynamics without accounting for such defects.

The before mentioned sublattices sites may be occupied by one of the three species uranium, aluminum or vacancies (v). If N is the number of lattice sites, then the number of sublattice sites is $N^U = N^{Al2} = N^{Al3} = N/5$ and $N^{Al1} = 2N/5$ where the superscript denotes the sublattice. In this way, each sublattice is occupied by $n_i^r$ atoms or vacancies ($r = U;Al1;Al2;Al3$ and $i = U;Al;v$). There are therefore three species for which the atomic concentrations on each sublattice are defined with respect to the total number of U and Al atoms $N_{at} = n_U + n_{Al}$ as $x_i^r = n_i^r/N_{at}$.

Within the frame of canonical ensemble the number of U and Al atoms is kept fixed but the total number N of lattice sites is variable and then the net concentration of vacancies $x_v = n_v/N_{at} = \sum_r x_v^r$ is also variable. The twelve atomic concentrations have to satisfy the following six constrains. The sum rule for concentrations on each sublattice given by:

$$\sum_i x_i^r - \frac{N^r}{N}\sum_r x_\nu^r = \frac{N^r}{N} \quad i = U;Al;v \quad r = U;Al1;Al2;Al3 \tag{1}$$

and the fixed atomic concentrations $x_U$ and $x_{Al}$ given by:

$$\sum_r x_{i\neq v}^r = x_i \quad i = U;Al \quad r = U;Al1;Al2;Al3 \tag{2}$$

However, among the Equations (1) and (2) only five are independent. We then choose the whole set (1) and the equation corresponding to $x_{Al}$ in the set (2).

According to the Wagner-Schottky model [22], the formation enthalpy (per atom) of an $UAl_4$ alloy with defects can be written as a linear function of point defect concentrations

$$\Delta H_{UAl_4}^d = \Delta H_{UAl_4}^0 + \sum_{i,r} H_i^r x_i^r \text{ with } H_U^U = H_{Al}^{Al_1} = H_{Al}^{Al_2} = H_{Al}^{Al_3} = 0 \tag{3}$$

$\Delta H_{UAl_4}^0$ is the formation enthalpy of perfect, defect free $UAl_4$, and $H_i^r$ are the defect formation enthalpies to be determined from first principles.

Assuming random distribution of point defects, the configurational entropy (per atom) is calculated using the mean-field approximation as

$$\begin{aligned}\Delta S_{conf} &= -k_B\left\{\sum_{i,r} x_i^r \ln x_i^r - \sum_r \frac{N^r}{N}(1+x_v) ln\left(\frac{N^r}{N}(1+x_v)\right)\right\} \\ &= -k_B\left\{\sum_{i,r} x_i^r \ln x_i^r - \frac{3}{5}(1+x_v) ln\left(\frac{1}{5}(1+x_v)\right)\right. \\ &\quad \left. - \frac{2}{5}(1+x_v) ln\left(\frac{2}{5}(1+x_v)\right)\right\}\end{aligned} \tag{4}$$

The concentrations of all the point defects in thermodynamic equilibrium can now be rigorously obtained through the minimization of the Gibbs free energy of the system: $\Delta G = \Delta H_f - T\Delta S_{conf}$. By differentiating the Gibbs energy with respect to the twelve unknowns and introducing five Lagrange multipliers corresponding to the chosen constrains (1) and (2), we obtain twelve equations involving the equilibrium atomic concentrations ($\beta = 1/k_BT$):

$$\frac{5^5 x_v^U \left(x_v^{Al1}\right)^2 x_v^{Al2} x_v^{Al3}}{2^2(1+x_v)^5} = exp\Big(-\beta\Big(H_v^U + 2H_v^{Al1} + H_v^{Al2} + H_v^{Al3}\Big)\Big) \tag{5a}$$

$$\frac{x_v^U x_U^{Al1}}{x_v^{Al1} x_U^U} = exp\Big(-\beta\Big(H_v^U + H_U^{Al1} - H_v^{Al1}\Big)\Big) \tag{5b}$$

$$\frac{x_v^U x_U^{Al2}}{x_v^{Al2} x_U^U} = exp\Big(-\beta\Big(H_v^U + H_U^{Al2} - H_v^{Al2}\Big)\Big) \tag{5c}$$

$$\frac{x_v^U x_U^{Al3}}{x_v^{Al3} x_U^U} = exp\Big(-\beta\Big(H_v^U + H_U^{Al3} - H_v^{Al3}\Big)\Big) \tag{5d}$$

$$\frac{x_v^{Al1} x_{Al}^U}{x_v^U x_{Al}^{Al1}} = exp\Big(-\beta\Big(H_v^{Al1} + H_{Al}^U - H_v^U\Big)\Big) \tag{5e}$$

$$\frac{x_v^{Al2} x_{Al}^U}{x_v^U x_{Al}^{Al2}} = exp\Big(-\beta\Big(H_v^{Al2} + H_{Al}^U - H_v^U\Big)\Big) \tag{5f}$$

$$\frac{x_v^{Al3} x_{Al}^U}{x_v^U x_{Al}^{Al3}} = exp\Big(-\beta\Big(H_v^{Al3} + H_{Al}^U - H_v^U\Big)\Big) \tag{5g}$$

$$x_{Al} = \frac{4}{5} + x_{Al}^U - x_U^{Al1} - x_U^{Al2} - x_U^{Al3} + \frac{1}{5}\Big(4x_v^U - x_v^{Al1} - x_v^{Al2} - x_v^{Al3}\Big) \tag{5h}$$

$$x_U^U = \frac{1}{5}\Big(1 - 4x_v^U + x_v^{Al1} + x_v^{Al2} + x_v^{Al3}\Big) - x_{Al}^U \tag{5i}$$

$$x_{Al}^{Al1} = \frac{2}{5}\Big(1 + x_v^U - \frac{3}{2}x_v^{Al1} + x_v^{Al2} + x_v^{Al3}\Big) - x_U^{Al1} \tag{5j}$$

$$x_{Al}^{Al2} = \frac{1}{5}\Big(1 + x_v^U + x_v^{Al1} - 4x_v^{Al2} + x_v^{Al3}\Big) - x_U^{Al2} \tag{5k}$$

$$x_{Al}^{Al3} = \frac{1}{5}\Big(1 + x_v^U + x_v^{Al1} + x_v^{Al2} - 4x_v^{Al3}\Big) - x_U^{Al2} \tag{5l}$$

A numerical solution of Eqs. (5a) – (5l) gives the equilibrium defect concentrations in $UAl_4$ at a given temperature and aluminum concentration $x_{Al}$. For displaying the results, it is more convenient to use the deviation from stoichiometry δ defined by:

$$x_{Al} = 4/5 + \delta \quad \text{or} \quad x_U = 1/5 - \delta \tag{6}$$

A first-principles supercell approach was employed to obtain the formation enthalpies of isolated point defects in $UAl_4$. We use both 80 and 120 atom supercells, each containing a single point defect. Details of all density functional theory (DFT) [23,24] calculations within the Vienna Ab initio Simulation Package (VASP) [25,26] used in the present work were described in a previous paper [15].

Supercell total energies ($E_T$) from spin-polarized first principles calculations were used to obtain the formation energies $\Delta E_f$ of $U_mAl_n$ compounds as:

$$\Delta E_f(U_mAl_n) = \frac{E_T(U_mAl_n) - mE_T(U) - nE_T(Al)}{m+n}$$

The reference states were pure U in the orthorhombic oC4 structure and pure Al in the cubic cF4 structure. The contribution of the pressure–volume term to the formation enthalpy of $U_mAl_n$ compounds at ordinary pressure is very small [16,17]. In the next sections we shall neglect this effect and consider that the defect formation enthalpies are equivalent to the defect formation energies.

## 3. Results and discussion

### 3.1. Point defect formation enthalpies

At T = 0 K, the point defect structure of an ordered compound is solely governed by enthalpy, and the point defects stable at this temperature are called constitutional defects.

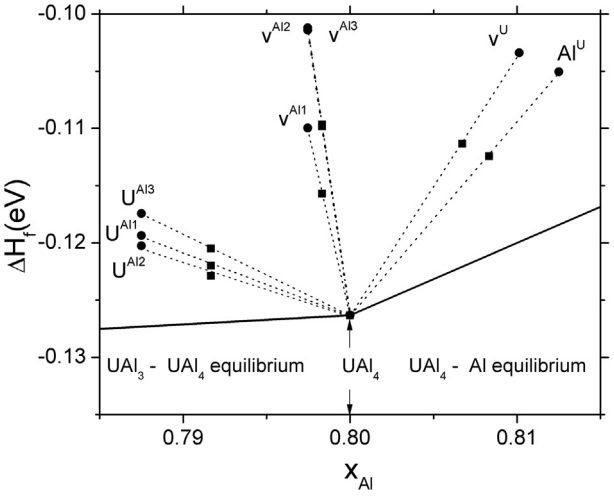


**Fig. 1.** Enthalpies of formation of the supercells 2 × 2 × 1 (●) and 3 × 2 × 1 (■) containing one defect.

In Fig. 1, the calculated formation enthalpies of off-stoichiometric $UAl_4$ alloys containing each of the eight possible types of point defects, the four antisites ($x_{Al}^U$, $x_U^{Al1}$, $x_U^{Al2}$ *and* $x_U^{Al3}$) and the four vacancies ($x_v^U$, $x_v^{Al1}$, $x_v^{Al2}$ *and* $x_v^{Al3}$), are plotted as different branches [15]. The branch giving the lowest formation enthalpy corresponds to the most stable defect structure; Fig. 1 thus shows that the constitutional point defects in Al-rich and U-rich $UAl_4$ are $Al^U$ antisites and $U^{Al2}$ antisites, respectively.

A linear relationship between $\Delta H_{UAl_4}^d$ and $x_{Al}$ as shown in Fig. 1 is predicted from Eqs. (3) and (5h) for each type of point defect. So, the defect formation enthalpies $H_i^r$ can be obtained from Fig. 1 slopes and they are listed in Table 1, for the eight point defects in $UAl_4$. These results were recently used to validate Modified Embedded Atom Method (MEAM) interatomic potentials fitted for Al and Al-U binary system [27].

Samples of $UAl_4$ characterized by other researchers were prepared by a peritectic reaction $UAl_3$ + *liquid Al* → Δ $UAl_4$ not completed [9–12] and so, the microstructure of the cast sample always consisted of two phases in equilibrium, $UAl_4$ and Al. Therefore and according to our results, the characterized samples would be Al rich alloys containing mainly $Al^U$ antisites. Taking this assumption, the ends of the range of densities measured (5.6 and 5.7 g/cm$^3$) and the volume of the unit cell reported by Refs. [12], we can predict a range of compositions for $UAl_4$ between 82.7 and 82.1 at.% Al which is in agreement with the reported range of measured compositions for the compound. This raw calculation can be done more accurate if all point defect concentrations at finite temperature are included.

**Table 1**
First-principles calculated formation enthalpies $H_i^r$ of isolated point defects in oI20 $UAl_4$.

| Point defect type | Designation | $H_i^r$(kJ/mol) | $H_i^r$(eV/atom) |
|---|---|---|---|
| Al antisite | $Al^U$ | 164 | 1.70 |
| U antisite1 | $U^{Al1}$ | 53 | 0.55 |
| U antisite2 | $U^{Al2}$ | 46 | 0.47 |
| U antisite3 | $U^{Al3}$ | 68 | 0.71 |
| U vacancy | $v^U$ | 174 | 1.81 |
| Al vacancy1 | $v^{Al1}$ | 124 | 1.29 |
| Al vacancy2 | $v^{Al1}$ | 190 | 1.97 |
| Al vacancy3 | $v^{Al1}$ | 191 | 1.98 |

The possibility of self interstitial occupancy has been analyzed, as they could deserve the addition of more sublattices to our model. As it was shown by Boucher [28], the $UAl_4$ structure can be presented as composed by blocks of five original $UAl_3$ (1 1 0) planes piled along the $UAl_4$ ⟨0 0 1⟩ axis with a reflection and a displacement of half a lattice parameter along <0 1 0> direction between blocks. In Fig. 2 the blocks are visually indicated by planes perpendicular to the z axis. Within blocks, the interstitial sites belong to the $L1_2$ ($UAl_3$) structure and they are named as 8i and 16j following the Wyckoff positions of the space group No. 74. At the reflection plane and in the ⟨100⟩ direction there appear two channel structures each surrounded by six rows of atoms (see Fig. 2a). In one channel, the rows contain only aluminum atoms. In the other channel, two rows containing only uranium atoms replace aluminum rows at both sides of the reflection plane. On the axis of both channels there are Wyckoff positions of the space group No. 74. These places look enough open so as to house interstitial atoms; we called them also with its Wyckoff position name i.e., 4d and 4c. Geometrical calculations were carried out in which the following Wigner-Seitz volumes of the proposed interstitials sites were obtained: 5.47 $Å^3$ (8i); 5.52 $Å^3$ (16j); 5.59 $Å^3$ (4c) and 5.75 $Å^3$ (4d). As expected the sites 4c and 4d are wider than the own sites of the structure $L1_2$, however all of them are about a third of the Wigner-Seitz volume of an aluminum atom in aluminum metal (16.52 $Å^3$). On the other hand, the Wigner-Seitz volume of a uranium atom in uranium metal is 20.75 $Å^3$ and then both antisites can be formed as our ab-initio calculations have shown. This discussion warns that the energy of formation of these self interstitials would be greater than that of the antisites and therefore, the influence of self interstitials on the thermodynamics of defects would be negligible as it was considered in this paper. Of course the issue must be clarified with ab-initio calculation of the energy of formation of these self-interstitials.

### 3.2. Defect concentrations

From the results in the precedent paragraph along with Eqs (5h) and (6), the concentrations of constitutional point defects ${}^{cons}x_i^r$ in the state of maximum ordering in off-stoichiometric $UAl_4$ are:

$$\delta > 0 \rightarrow {}^{cons}x_{Al}^{U} = \delta \tag{7a}$$

for Al-rich region; and

$$\delta < 0 \rightarrow {}^{cons}x_{U}^{Al2} = |\delta| \tag{7b}$$

for U-rich region.

The thermal point defects ${}^{th}x_i^r$ appear at finites temperatures in addition to the constitutional point defects. Since the alloy composition is fixed, the condition given by Eq. (5h) rules the total number of point defect concentrations. In particular, the total point defect concentrations of the same type as the constitutional point defects given by

$$x_{Al}^{U} = {}^{cons}x_{Al}^{U} + {}^{th}x_{Al}^{U} \tag{8a}$$

$$x_{U}^{Al2} = {}^{cons}x_{U}^{Al2} + {}^{th}x_{U}^{Al2} \tag{8b}$$

can be a positive number even when their thermal concentration is a negative number (as in the case of annihilation of defects with increasing temperature). Instead of this, for all other kind of point defects the total and thermal concentrations are equal.

Substituting Eqs. (6)–(8) into Eq. (5h) the condition for the thermal point defect concentrations becomes:

$$\begin{aligned} &{}^{th}x_{Al}^{U} - {}^{th}x_{U}^{Al1} - {}^{th}x_{U}^{Al2} - {}^{th}x_{U}^{Al3} + \frac{1}{5}\left(4\,{}^{th}x_{v}^{U} - {}^{th}x_{v}^{Al1} - {}^{th}x_{v}^{Al2}\right. \\ &\left. - {}^{th}x_{v}^{Al3}\right) \\ &= 0 \end{aligned} \tag{9}$$

It follows from Eq. (9) that thermal defects are only possible as combinations of point defects with the constraint of composition (*composition-conserving defect* (CD) [29]).

There are twelve simplest CD consisting of two types of point defects which can be thermally activated in the maximally ordered alloy of any composition including the defect-free stoichiometric alloy. These can be obtained from Eq. (9) considering the case when all the thermal point defect concentrations are positive numbers. Table 2 lists the reactions together with their reaction enthalpies calculated from the formation enthalpies $H_i^r$ of isolated point defects in Table 1.

As mentioned above, the thermal point defect concentrations of the same type as the constitutional point defects can be negative numbers and there are additional possibilities to satisfy Eq. (9) by replacing the constitutional antisites by vacancies or other types of antisites. This means that the formation of a defect between

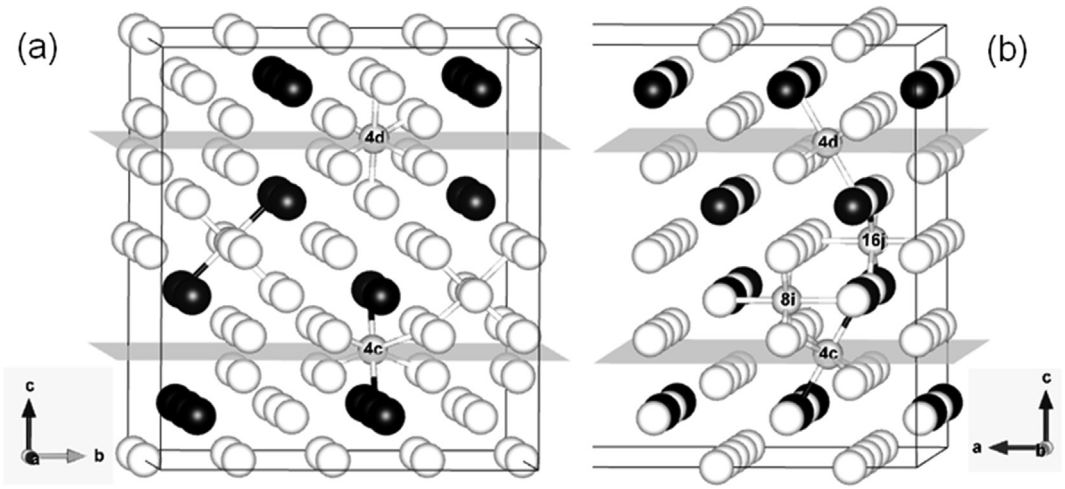


**Fig. 2.** Proposed interstitials sites in the oI20 ($UAl_4$) structure. a) View in the ⟨100⟩ direction, b) View in the ⟨010⟩ direction.

**Table 2**
Calculated formation enthalpies $H_D$ of typical composition-conserving defects in $UAl_4$. $N_d$ is the number of point defects generated through the reaction.

| Reaction | Enthalpy | Equilibrium equation | $H_d$ (eV) | $H_d/N_d$ (eV/def) |
|---|---|---|---|---|
| $0 \rightarrow U^{Al1} + Al^U$ | $H_{2D1} = H^U_{Al} + H^{Al1}_U$ | $\frac{x^U_{Al}x^{Al1}_U}{x^{Al1}_{Al}x^U_U} = \exp\{-\beta H_{2D1}\}$ | 2.25 | 1.12 |
| $0 \rightarrow U^{Al2} + Al^U$ | $H_{2D2} = H^U_{Al} + H^{Al2}_U$ | $\frac{x^U_{Al}x^{Al2}_U}{x^{Al2}_{Al}x^U_U} = \exp\{-\beta H_{2D2}\}$ | 2.17 | 1.09 |
| $0 \rightarrow U^{Al3} + Al^U$ | $H_{2D3} = H^U_{Al} + H^{Al3}_U$ | $\frac{x^U_{Al}x^{Al3}_U}{x^{Al3}_{Al}x^U_U} = \exp\{-\beta H_{2D3}\}$ | 2.40 | 1.20 |
| $0 \rightarrow v^U + 4v^{Al1}$ | $H_{5D1} = H^U_v + 4H^{Al1}_v$ | $\frac{5^5 x^U_v (x^{Al1}_v)^4 x^{Al2}_{Al} x^{Al3}_{Al}}{2^2(1+x_v)^5 (x^{Al1}_{Al})^2} = \exp\{\{-\beta H_{5D1}\}\}$ | 6.96 | 1.39 |
| $0 \rightarrow v^U + 4v^{Al2}$ | $H_{5D2} = H^U_v + 4H^{Al2}_v$ | $\frac{5^5 x^U_v (x^{Al2}_v)^4 (x^{Al1}_{Al})^2 x^{Al3}_{Al}}{2^2(1+x_v)^5 (x^{Al2}_{Al})^3} = \exp\{-\beta H_{5D2}\}$ | 9.68 | 1.94 |
| $0 \rightarrow v^U + 4v^{Al3}$ | $H_{5D3} = H^U_v + 4H^{Al3}_v$ | $\frac{5^5 x^U_v (x^{Al3}_v)^4 (x^{Al1}_{Al})^2 x^{Al2}_{Al}}{2^2(1+x_v)^5 (x^{Al3}_{Al})^3} = \exp\{-\beta H_{5D3}\}$ | 9.74 | 1.95 |
| $0 \rightarrow Al^U + 5v^{Al1}$ | $H_{6D1} = H^U_{Al} + 5H^{Al1}_v$ | $\frac{5^5 x^U_{Al} (x^{Al1}_v)^5 x^{Al2}_{Al} x^{Al3}_{Al}}{2^2(1+x_v)^5 (x^{Al1}_{Al})^3} = \exp\{-\beta H_{6D1}\}$ | 8.14 | 1.36 |
| $0 \rightarrow Al^U + 5v^{Al2}$ | $H_{6D2} = H^U_{Al} + 5H^{Al2}_v$ | $\frac{5^5 x^U_{Al} (x^{Al2}_v)^5 (x^{Al1}_{Al})^2 x^{Al3}_{Al}}{2^2(1+x_v)^5 (x^{Al2}_{Al})^4} = \exp\{-\beta H_{6D2}\}$ | 11.54 | 1.92 |
| $0 \rightarrow Al^U + 5v^{Al3}$ | $H_{6D3} = H^U_{Al} + 5H^{Al3}_v$ | $\frac{5^5 x^U_{Al} (x^{Al3}_v)^5 (x^{Al1}_{Al})^2 x^{Al2}_{Al}}{2^2(1+x_v)^5 (x^{Al3}_{Al})^4} = \exp\{-\beta H_{6D3}\}$ | 11.62 | 1.94 |
| $0 \rightarrow 4U^{Al1} + 5v^U$ | $H_{9D1} = 4H^{Al1}_U + 5H^U_v$ | $\frac{5^5 (x^U_v)^5 (x^{Al1}_U)^4 x^{Al2}_{Al} x^{Al3}_{Al}}{2^2(1+x_v)^5 (x^U_U)^4 (x^{Al1}_{Al})^2} = \exp\{-\beta H_{9D1}\}$ | 11.24 | 1.25 |
| $0 \rightarrow 4U^{Al2} + 5v^U$ | $H_{9D2} = 4H^{Al2}_U + 5H^U_v$ | $\frac{5^5 (x^U_v)^5 (x^{Al2}_U)^4 (x^{Al1}_{Al})^2 x^{Al3}_{Al}}{2^2(1+x_v)^5 (x^{Al2}_{Al})^3 (x^U_U)^4} = \exp\{-\beta H_{9D2}\}$ | 10.93 | 1.21 |
| $0 \rightarrow 4U^{Al3} + 5v^U$ | $H_{9D3} = 4H^{Al3}_U + 5H^U_v$ | $\frac{5^5 (x^U_v)^5 (x^{Al3}_U)^4 (x^{Al1}_{Al})^2 x^{Al2}_{Al}}{2^2(1+x_v)^5 (x^U_U)^4 (x^{Al3}_{Al})^3} = \exp\{-\beta H_{9D3}\}$ | 11.87 | 1.32 |

**Table 3**
Calculated formation enthalpies $H_D$ of *interbranch* defects reactions. $N_d$ stands for the number of defects generated through the reaction.

| Reaction | Enthalpy | Equilibrium equation | $H_d$ (eV) (eV) | $H_d/N_d$ (eV/def) |
|---|---|---|---|---|
| $4Al^U \rightarrow 5v^U$ | $H_{IU} = 5H^U_v - 4H^U_{Al}$ | $\frac{5^5 (x^U_v)^5 (x^{Al1}_{Al})^2 x^{Al2}_{Al} x^{Al3}_{Al}}{2^2(1+x_v)^5 (x^U_{Al})^4} = \exp\{-\beta H_{IU}\}$ | 2.25 | 0.45 |
| $U^{Al2} \rightarrow 5v^{Al2}$ | $H_{IAl2} = 5H^{Al2}_v - H^{Al2}_U$ | $\frac{5^5 (x^{Al2}_v)^5 (x^{Al1}_{Al})^2 x^{Al3}_{Al} x^U_U}{2^2(1+x_v)^5 x^{Al2}_U (x^{Al2}_{Al})^3} = \exp\{-\beta H_{IAl2}\}$ | 9.37 | 1.87 |
| $U^{Al2} \rightarrow 5v^{Al3}$ | $H_{IAl23} = 5H^{Al3}_v - H^{Al2}_U$ | $\frac{5^5 (x^{Al3}_v)^5 x^U_U (x^{Al1}_{Al})^2 (x^{Al2}_{Al})^2}{2^2(1+x_v)^5 x^{Al2}_U (x^{Al3}_{Al})^4} = \exp\{-\beta H_{IAl23}\}$ | 9.37 | 1.87 |
| $U^{Al2} \rightarrow 5v^{Al1}$ | $H_{IAl21} = 5H^{Al1}_v - H^{Al2}_U$ | $\frac{5^5 (x^{Al1}_v)^5 x^U_U (x^{Al2}_{Al})^2 x^{Al3}_{Al}}{2^2(1+x_v)^5 x^{Al2}_U (x^{Al1}_{Al})^3} = \exp\{-\beta H_{IAl21}\}$ | 5.97 | 1.19 |
| $U^{Al2} \rightarrow U^{Al3}$ | $H_{IAl2Al3} = H^{Al3}_U - H^{Al2}_U$ | $\frac{x^{Al3}_U x^{Al2}_{Al}}{x^{Al2}_U x^{Al3}_{Al}} = \exp\{-\beta H_{IAl2Al3}\}$ | 0.23 | 0.23 |
| $U^{Al2} \rightarrow U^{Al1}$ | $H_{IAl2Al1} = H^{Al1}_U - H^{Al2}_U$ | $\frac{x^{Al1}_U x^{Al2}_{Al}}{x^{Al2}_U x^{Al1}_{Al}} = \exp\{-\beta H_{IAl2Al1}\}$ | 0.08 | 0.08 |

branches is accompanied by the annihilation of the constitutional defect. This type of CD is called *interbranch* defect [24]. The point defect reactions leading to interbranch CD in $UAl_4$ are shown in Table 3 for the both Al-rich and U-rich regions.

Both Tables 2 and 3 include the equilibrium relationship between concentrations of point defects involved in each reaction. These equilibrium relations are obtained from the equilibrium Equation (5) after suitable algebraic calculations.

A comparison between the values of formation enthalpies by defect in Tables 2 and 3 allows us to decide about the most favorable defects reactions. For the stoichiometric compound only the reactions in Table 2 can be chosen, so the dominating reaction is $H_{2D2}$ where the thermal defect made up of the antisites $Al^U$ and $U^{Al2}$ is formed from the perfect crystal. In the rich uranium zone the most favorable reaction is $H_{IAl2Al1}$, the thermal defect is in consequence an *interbranch* defect where a $U^{Al2}$ antisite is replaced by a $U^{Al1}$ antisite. In the rich aluminum zone the most favorable reaction is $H_{IU}$, and the thermal defect is an *interbranch* where four antisite aluminum atoms are replaced by five uranium vacancies.

Fig. 3 presents the point defect concentrations in $UAl_4$ as function of composition at 823 K and 1000 K. These results are obtained by solving the set of Eqs. (5a) – (5l) with the values of the formation enthalpies $H^r_i$ of isolated point defects in Table 1. The resolution is performed by successive iterations from a realistic initial guess of the defect concentrations until the required precision is reached. As expected from our previous analysis, the constitutional point defect is the predominant defect in the off-stoichiometric zone and the predominant thermal defect is that coming from the most favorable defect reaction in that composition zone. For example, in the rich uranium zone the predominant point defects are the $U^{Al2}$ antisites followed by the $U^{Al1}$ antisites. The downward sequence of the other thermal defect concentrations is harder to predict due to the relationships between the different CD's. In the next paragraph we discuss these relationships in the context of the effective defect formation energy concept.

Now we can return to the discussion about the density of the compound $UAl_4$. A rigorous formula for the density of $UAl_4$ including concentrations of point defects is as follows

$$\rho = \frac{20}{N_A V_{cell}(1+x_v)}(x_{Al}M_{Al} + x_U M_U)$$

where $N_A$ is the Avogadro number, $V_{cell}$ is the unit cell volume, $M_{Al}$ and $M_U$ the atomic mass. From Fig. 3 is clear that the amount of total vacancy concentration is always negligible in front to the unit, so the density is dominated by the antisite defect concentration as was discussed before.

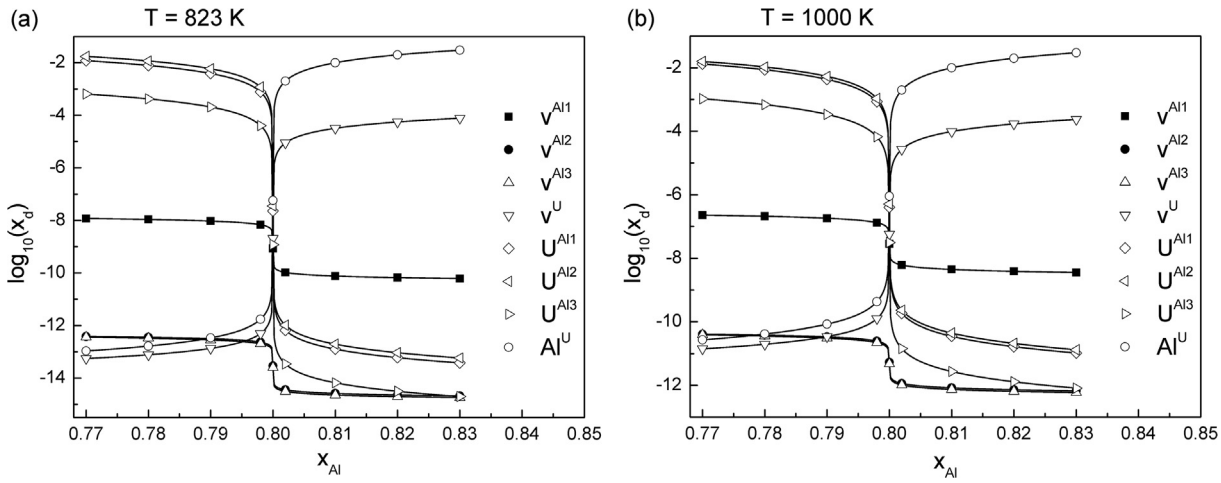


**Fig. 3.** Equilibrium point defect concentrations $x_d$ as a function of Al composition at **(a)** T = 823 K. **(b)** T = 1000 K.

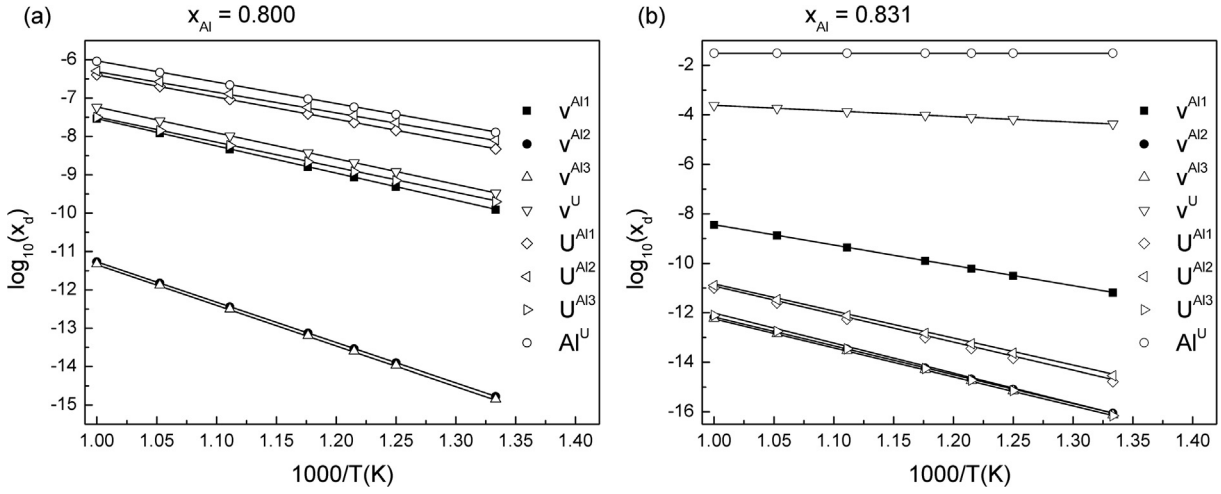


**Fig. 4.** Arrhenius plot of equilibrium point defect concentrations $x_d$; symbols: calculated using the set of and ; lines: estimated with the values of effective defect enthalpy given in Table 4.

**Table 4**
Values of the effective enthalpies and pre-exponential factors or the Arrhenius law of point defects concentrations in stoichiometric and Al-rich $UAl_4$ compound.

| Defect | $\delta = 0.0$ | | | | Defect | $\delta = 0.031$ | | | |
|---|---|---|---|---|---|---|---|---|---|
| | $H_d^{eff}$ (eV) | | $x_d^{\infty}$ | | | $H_d^{eff}$ (eV) | | $x_d^{\infty}$ | |
| | Num[a] | aprox[b] | num[a] | aprox[b] | | num[a] | aprox[b] | num[a] | aprox[b] |
| $Al^U$ | 1.10 | 1.10 | 0.32 | 0.35 | $Al^U$ | 0.00 | 0.00 | 0.03 | 0.03 |
| $U^{Al2}$ | 1.07 | 1.07 | 0.13 | 0.12 | $v^U$ | 0.45 | 0.45 | 0.04 | 0.05 |
| $U^{Al1}$ | 1.15 | 1.14 | 0.25 | 0.23 | $v^{Al1}$ | 1.63 | 1.63 | 0.58 | 0.58 |
| $v^U$ | 1.33 | 1.33 | 0.29 | 0.31 | $U^{Al2}$ | 2.17 | 2.17 | 1.11 | 1.29 |
| $U^{Al3}$ | 1.31 | 1.30 | 0.13 | 0.12 | $U^{Al1}$ | 2.25 | 2.25 | 2.23 | 2.58 |
| $v^{Al1}$ | 1.41 | 1.41 | 0.36 | 0.36 | $U^{Al3}$ | 2.41 | 2.40 | 1.11 | 1.29 |
| $v^{Al2}$ | 2.09 | 2.09 | 0.18 | 0.18 | $v^{Al2}$ | 2.31 | 2.31 | 0.29 | 0.29 |
| $v^{Al3}$ | 2.10 | 2.10 | 0.18 | 0.18 | $v^{Al3}$ | 2.32 | 2.32 | 0.29 | 0.29 |

[a] Linear least squares fit of the $x_d$ values (symbols) in Fig. 4.
[b] Calculated using the analytical expressions given in Table 5.

### 3.3. Effective defect enthalpies

The numerical resolution of the set of Eqs. (5a)–(5l) can be also done at fix aluminum composition as a function of temperature. In Fig. 4 we plot the defect concentrations obtained for the stoichiometric compound and for an aluminum rich off-stoichiometric compound in the temperature range of 750 K–1000 K. It can be seen that the point defect concentrations in $UAl_4$ do exhibit Arrhenius temperature dependence. This pseudo Arrhenius law allows us to obtain the effective formation enthalpies of isolated point defects in $UAl_4$ through a linear fit according to the relationship $x_d = x_d^{\infty} exp\{-H_d^{eff}/(k_B T)\}$. Our results are presented in

**Table 5**
Approximate analytical expressions of the effective enthalpies and pre-exponential factors for the Arrhenius law of point defects concentrations in stoichiometric and Al-rich $UAl_4$ compound.

| Defect | $\delta = 0$ | | Defect | $\delta > 0$ | |
|---|---|---|---|---|---|
| | $H_d^{eff}$ | $x_d^{\infty}$ | | $H_d^{eff}$ | $x_d^{\infty}$ |
| $Al^U$ | $\frac{H_{2D1}+H_{2D2}}{4}$ | $\frac{\sqrt{3}}{5}$ | $Al^U$ | 0 | $\delta$ |
| $U^{Al2}$ | $H_{2D2} - \frac{H_{2D1}+H_{2D2}}{4}$ | $\frac{1}{5\sqrt{3}}$ | $v^U$ | $\frac{H_{IU}}{5}$ | $\sqrt[5]{\frac{\delta^4}{5}}$ |
| $U^{Al1}$ | $H_{2D1} - \frac{H_{2D1}+H_{2D2}}{4}$ | $\frac{2}{5\sqrt{3}}$ | $v^{Al1}$ | $\frac{H_{6D1}}{5}$ | $\frac{2}{5\sqrt[5]{5\delta}}$ |
| $v^U$ | $\frac{1}{5}\left[H_{9D2} - 4\left(H_{2D2} - \frac{H_{2D1}+H_{2D2}}{4}\right)\right]$ | $\frac{3^{2/5}}{5}$ | $U^{Al2}$ | $H_{2D2}$ | $\frac{1}{5^2\delta}$ |
| $U^{Al3}$ | $H_{2D3} - \frac{H_{2D1}+H_{2D2}}{4}$ | $\frac{1}{5\sqrt{3}}$ | $U^{Al1}$ | $H_{2D1}$ | $\frac{2}{5^2\delta}$ |
| $v^{Al1}$ | $\frac{1}{5}\left(H_{6D1} - \frac{H_{2D1}+H_{2D2}}{4}\right)$ | $\frac{2}{5\sqrt[10]{3}}$ | $U^{Al3}$ | $H_{2D3}$ | $\frac{1}{5^2\delta}$ |
| $v^{Al2}$ | $\frac{1}{5}\left(H_{6D2} - \frac{H_{2D1}+H_{2D2}}{4}\right)$ | $\frac{1}{5\sqrt[10]{3}}$ | $v^{Al2}$ | $\frac{H_{6D2}}{5}$ | $\frac{1}{5\sqrt[5]{5\delta}}$ |
| $v^{Al3}$ | $\frac{1}{5}\left(H_{6D3} - \frac{H_{2D1}+H_{2D2}}{4}\right)$ | $\frac{1}{5\sqrt[10]{3}}$ | $v^{Al3}$ | $\frac{H_{6D3}}{5}$ | $\frac{1}{5\sqrt[5]{5\delta}}$ |

Table 4. The introduction of effective defect enthalpy of formation arises from the fact that the experimental data is frequently interpreted using a formalism based on the Arrhenius formula. Hereinafter, the results for the uranium rich off-stoichiometric compounds are omitted since they are not observed experimentally.

If certain conditions are fulfilled, Eqs. (5a)–(5l) can be further simplified to give approximate analytical solutions, which thus allows for a direct interpretation of the physical meaning of the effective defect formation energies. Specifically, such conditions are: (i) in stoichiometric $UAl_4$, we can see from Fig. 4a that the point defect concentrations $x_{Al}^{U}$, $x_{U}^{Al1}$ and $x_{U}^{Al2}$ strongly dominates over the entire temperature range and they are a product of the CD thermal defects with enthalpies $H_{2D1}$ and $H_{2D2}$. Then, assuming negligible the other concentrations of point defects and by using the equilibrium equations $H_{2D1}$ and $H_{2D2}$ of Table 2, one obtains the Arrhenius relationship for the dominant concentrations with the effective enthalpies and pre-exponential factors listed in Table 5. The other point defect concentrations are obtained using the remaining equilibrium equations in a downward sequence given by the values of the reaction enthalpies of Table 2. (ii) in the off-stoichiometric compounds, as it can be seen in Fig. 4b, the concentration of the constitutional defect is much larger than those of thermal defects and can be considered as temperature independent. In addition, one employs the same methodology used in the stoichiometric compound but should include the interbranch defect $H_{IU}$ in the analysis.

All our derived analytical expressions for the connections between $H_d^{eff}$ and the formation enthalpies of the composition-conserving and interbranch defects in $UAl_4$ are presented in the Table 5. We note that such analytical expressions give results in excellent agreement with those obtained from numerical fitting (see Table 4). Also, we conclude that the $H_d^{eff}$ in $UAl_4$ generally contain information of other point defects, not just defects of type d. As a result, they no longer have the simple physical meaning as in monoatomic crystals.

### 3.4. Migration

Based on our results, we can suggest that the aluminum rich off stoichiometric $UAl_4$ experimentally observed can be explained by substitutional disorder at low temperatures. At higher temperatures, two main reactions are predicted where the aluminum antisite concentration is preserved by generating uranium and Al1 vacancies. If this is the case, diffusion by vacancies could only take place by thermal vacancies mechanism, since no constitutional vacancies would exist.

We can go back now to the growth of $UAl_4$ phase in an $UAl_3$/Al diffusion couple. If we apply the $Cu_3Au$ rule [30], the mobile atom should be Al as it is the majority element. This assumption is supported by experimental evidence as we have already analyzed in a previous report [6]. The process would take place by diffusion of Al atoms from Al to $UAl_3$ side traveling along of the $UAl_4$ compound. Aluminum diffusion can be assumed to be related to vacancy diffusion towards the opposite direction. Taking into account our results, we analyze the possible vacancy migration mechanisms in the $UAl_4$ compound from the minimum jump distances and the maximum probability of finding the defect complex created during the jump [31].

From Fig. 4b) it is clear that for an aluminum rich off-stoichiometric $UAl_4$ compound in the temperature range of 750 K–1000 K the main point defect concentrations are those for $Al^U$, $v^U$ and $v^{Al1}$. These point defects are located on two sublattices whose spatial arrangement is shown in Fig. 5a). This arrangement looks like a channel with hexagonal wall running along the **a** axis. The hexagonal wall is formed by two kinds of planes, one containing only atoms of Al1 sublattice while the other contains atoms of both Al1 and U sublattices (see Fig. 5b).

The next nearest-neighbor (NNN) jumps are between the Al1 sites while the nearest-neighbor (NN) jumps are between the Al1 and U sites. In the NNN jump, as shown in Fig. 6, exchanges of atoms with vacancies are confined to the same sublattice so that the diffusion of Al is independent of the concentration of point defects other than $v^{Al1}$. In the NN jumps the vacancies on one sublattice exchange with the "normal" or "antistructure" ("antisite") atoms on the other sublattice, then any operative diffusion mechanism must contain a series of NN jumps that results in net atom movements but also retains the degree of order of the material. Defect complexes of various sizes will be created and destroyed during this series of NN jumps. Therefore the diffusion coefficients contributed by a specific mechanism should also be proportional to the probability of finding those defect complexes associated with the mechanism. Two recognized mechanisms proposed for diffusion in intermetallic compounds [32,33] are consistent with our results, namely, triple-defect (TD) mechanism [34] and antistructure bridge (ASB) mechanism [26]. Graphical representation of both mechanisms is also displayed in Fig. 6.

To a first approximation the probability of finding a two-defect complex such as those of the TD and ASB mechanisms is proportional to the product of the concentrations of these two defects. Accordingly, the contribution to the diffusion of Al atoms from these mechanisms should be

$$D_{Al}(NNN) \propto x_{v^{Al1}} \qquad D_{Al}(ASB) \propto x_{Al^U} \times x_{v^U} \qquad D_{Al}(TD) \propto x_{v^{Al1}} \times x_{v^U}$$

The Fig. 7 shows the temperature dependence of $D_{Al}$ for the data in Fig. 4b) ($x_{Al} = 0.831$ or $\delta = 0.031$). As it can be seen, the contribution of the ASB mechanism to the value of *log* ($D_{Al}$) at every temperature within the range is much greater than that of the other mechanisms. This means that the energy of diffusion of Al in the compound should be at least equal to the effective formation enthalpy of the uranium vacancy given in Table 4. The calculation of migration energies involved in the ASB mechanism will be the subject of our next work.

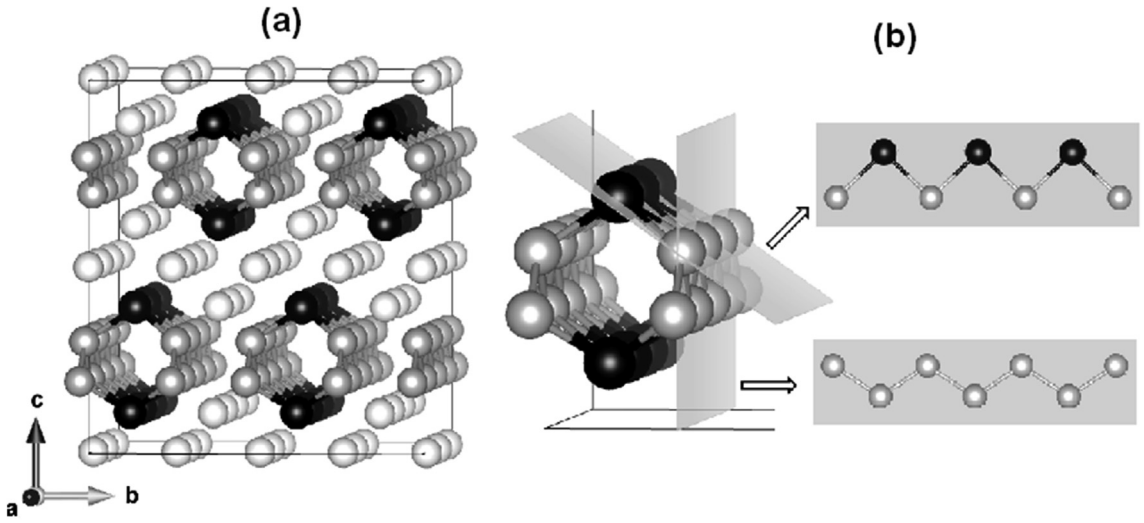


**Fig. 5.** (a) Crystal structure of $UAl_4$. Black circles denote the U sites and circles colored with dark gray shade indicate Al1 sites. The other Al sites are colored with light gray shade. (b) Detail of the planes containing the next nearest-neighbor (gray bonding) and the nearest-neighbor (black-gray bonding) atom sites.

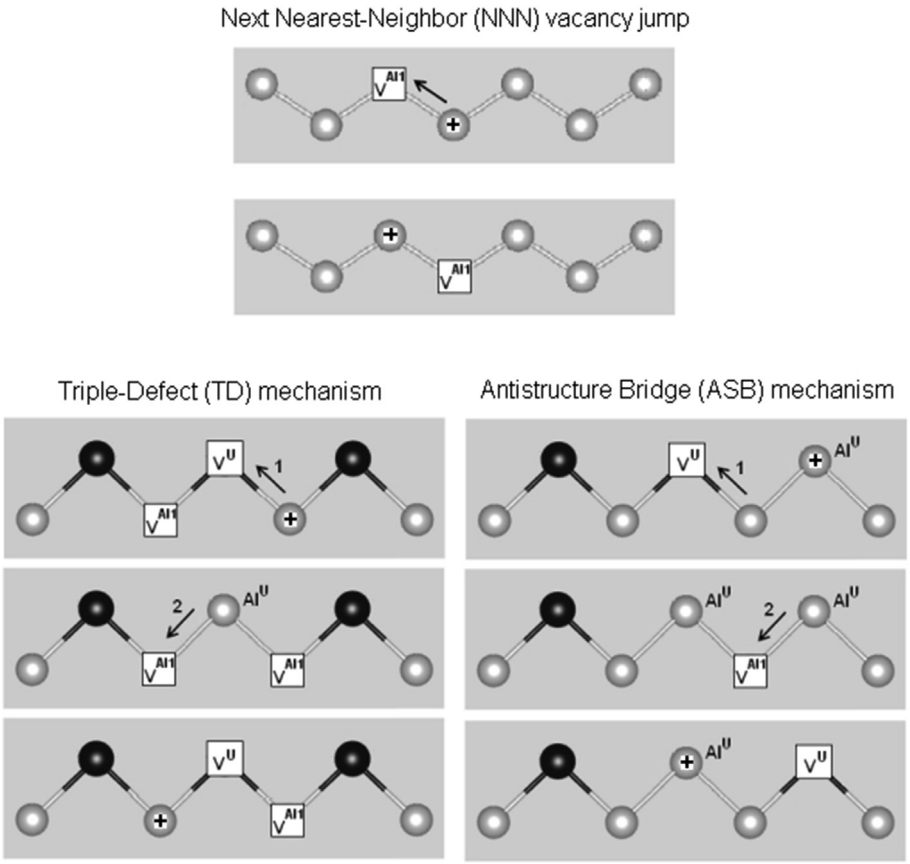


**Fig. 6.** Schematic presentation of the migration mechanisms proposed for Al diffusion in the aluminum rich off stoichiometric $UAl_4$ intermetallic compound.

## 4. Conclusions

In this work, we have developed a defect statistical model in the canonical ensemble for $AB_4$ phases where four sublattices are necessary to account for the structure of the phase and we applied this model to the oI20 $UAl_4$ phase. We obtained the formation enthalpies of the eight possible point defects, vacancies and antisites in each sublattice, from our already published ab initio calculations of total energy of oI20 $UAl_4$ supercells containing one of the possible point defects. These values were used in a Wagner-Schottky model to calculate the formation enthalpy of an $UAl_4$ alloy with defects.

Our results show that uranium antisite in the Al2 site and aluminum antisite are the constitutional point defects on the Al-

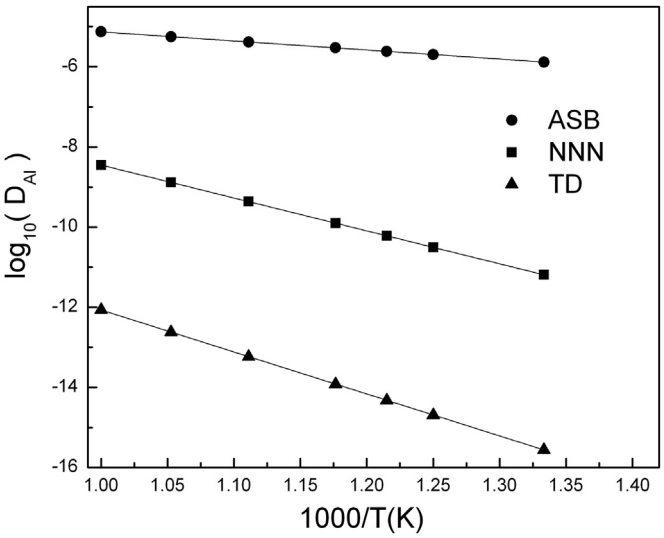


**Fig. 7.** Contributions to the diffusion coefficient of Al atoms in terms of the NNN vacancy jump, ASB and TD mechanisms for the aluminum rich off-stoichiometric $UAl_4$ intermetallic compound.

depleted and Al-rich sides of stoichiometry, respectively. For stoichiometric $UAl_4$, the dominant thermal defect is made up of the antisites $Al^U$ and $U^{Al2}$. At both sides of stoichiometry the dominant thermal defects are interbranch defects, in the rich uranium zone a constitutional antisite uranium atom ($U^{Al2}$) is replaced by an antisite uranium atom ($U^{Al1}$) while in the rich aluminum zone four constitutional antisite aluminum atoms ($Al^U$) are replaced by five uranium vacancies.

Finally, the point defects effective formation energies are obtained for the stoichiometric as well as for the Al-rich off-stoichiometric alloy. These results allow us to identify the antistructure bridge (ASB) mechanism as the most probable for the diffusion for Al atoms in the Al-rich $UAl_4$ intermetallic compound. In our analysis only the formation energy of the defect complexes that are required for diffusion is considered. Moreover, it is assumed that the change in the migration energy with the structure of the defect complexes is lower than the change of the formation energy.

## Acknowledgements

This work was partially supported by Gerencia Materiales of the Comisión Nacional de Energía Atómica, Argentina; ANPCyT under grant PICT-2011-1861 and UNSAM under grant C063.

## References

[1] W. Dienst, S. Nazare, F. Thummler, Irradiation behaviour of $UAl_x$-Al dispersion fuels for thermal high flux reactors, J. Nucl. Mater. 64 (1977) 1–13.
[2] G.L. Hofman, J. Rest, J.L. Snelgrove, T. Wiencek, S. Koster van Groos, Aluminum-$U_3Si_2$ interdifussion and its implications for the performance of highly loaded fuel operating at higher temperatures and fission rates, in: Proceedings of RERTR-1996 International Meeting on Reduced Enrichment for Research and Test Reactors, Korea, Seoul, October 1996.
[3] Y.S. Kim, G.L. Hofman, H.J. Ryu, J.M. Park, A.B. Robinson, D.M. Wachs, Modeling of interaction layer growth between U-Mo particles and an Al matrix, Nucl. Eng. Technol. 45 (2013) 827–838.
[4] S. Balart, L. Kniznik, C. Komar Varela, P.H. Gargano, M. Mirandou, S. Aricó, P.R. Alonso, G.H. Rubiolo, A. Fortis, L. Gribaudo, Current activities in the out of pile investigations of the interaction between UMo and Al or Al alloys, in: Proceedings of RERTR-2009 International Meeting on Reduced Enrichment for Research and Test Reactors, China, Beijing, November 2009.
[5] M.E. Kassner, P.H. Adler, M.G. Adamson, D.E. Peterson, Evaluation and thermodynamic analysis of phase equilibria in the U-Al system, J. Nucl. Mater. 167 (1989) 160–168.
[6] L. Kniznik, P.R. Alonso, P.H. Gargano, G.H. Rubiolo, Simulation of $UAl_4$ growth in an $UAl_3$/Al diffusion couple, J. Nucl. Mater. 414 (2011) 309–315.
[7] B. Sundman, B. Jansson, J.-O. Andersson, The Thermo-Calc databank system, CalPhaD 9 (1985) 153–190.
[8] J.-O. Andersson, L. Höglund, B. Jönsson, J. Agren, Computer simulation of multicomponent diffusional transformations in steel, in: G.R. Purdy (Ed.), Fundamentals and Applications of Ternary Diffusion, Pergamon Press, New York, 1990, pp. 153–163.
[9] B.S. Borie, Crystal structure of $UAl_4$, Trans. AIME 191 (1951) 800–802.
[10] O.J.C. Runnalls, R.R. Boucher, Transformations in $UAl_4$ and $PuAl_4$, Trans. AIME 233 (1965) 1726–1732.
[11] V.Y. Zenou, G. Kimmel, C. Cotler, M. Aizenshtein, Structure of $UAl_4$ prepared by solid state reaction, J. Alloy Comp. 329 (2001) 189–194.
[12] O. Tougait, H. Noël, Stoichiometry of $UAl_4$, Intermetallics 12 (2004) 219–223.
[13] M.E. Kassner, P.H. Adler, M.G. Adamson, D.E. Peterson, Evaluation and thermodynamic analysis of phase equilibria in the U-Al system, J. Nucl.Mater. 167 (1989) 160–168.
[14] P. Villars, L.D. Calvert, Pearson's handbook of crystallographic data for intermetallic phases, in: ASM International, second ed., vol. 2, Materials Park, Ohio, 1991.
[15] L. Kniznik, P.R. Alonso, P.H. Gargano, G.H. Rubiolo, Energetics and electronic structure of $UAl_4$ with point defects, J. Nucl. Mater. 466 (2015) 539–550.
[16] C. Colinet, J.-C. Tedenac, S.G. Fries, constitutional and thermal defects in $D0_{19}$-$SnTi_3$, Intermetallics 16 (2008) 923–932.
[17] C. Colinet, J.-C. Tedenac, constitutional and thermal defects in $B8_2$–$SnTi_2$, Intermetallics 17 (2008) 291–304.
[18] M.O. Zacate, G.S. Collins, Composition-driven changes in lattice sites occupied by indium solutes in $Ni_2Al_3$ phases, Phys. Rev. B 70 (2004) 024202.
[19] D. Tingaud, R. Besson, Point defects and diffusion in ordered alloys: an ab initio study of the effect of vibrations, Intermetallics 45 (2014) 38–45.
[20] C. Colinet, J.C. Tedenac, Structural stability of intermetallic phases in the Si–Ti system. Point defects and chemical potentials in $D8_8$-$Si_3Ti_5$ phase, Intermetallics 18 (2010) 1444–1454.
[21] D. Tingaud, F. Nardou, Diffusion in complex ordered alloys: atomic-scale investigation of $NiAl_3$, Phys. Rev. B 81 (2010) 174108.
[22] C. Wagner, Thermodynamics of Alloys, first ed., Addison-Wesley, Cambridge, Massachusetts, 1952.
[23] P. Hohenberg, W. Kohn, Inhomogeneous electron gas, Phys. Rev. 136 (1964) B864–B871.
[24] W. Kohn, L.J. Sham, Self-consistent equations including exchange and correlation effects, Phys. Rev. 140 (1965) A1133–A1138.
[25] G. Kresse, J. Furthmüller, Efficiency of ab-initio total energy calculations for metals and semiconductors using a plane-wave basis set, Comp. Mater. Sci. 6 (1996) 15–50.
[26] G. Kresse, J. Furthmüller, Efficient iterative schemes for ab initio total-energy calculations using a plane-wave basis set, Phys. Rev. B 54 (1996) 11169–11186.
[27] M.I. Pascuet, J.R. Fernández, Atomic interaction of the MEAM type for the study of intermetallics in the Al-U alloy, J. Nucl.Mater. 467 (2015) 229–239.
[28] R. Boucher, Etude des alliages aluminium-uranium application a la transformation a l'etat solide $UAl_3 \rightarrow UA1_4$, J. Nucl.Mater. 1 (1969) 13–27.
[29] P.A. Korzhavyi, A.V. Ruban, A.Y. Lozovoi, YuKh Vekilov, I.A. Abrikosov, B. Johansson, Constitutional and thermal point defects in B2 NiAl, Phys. Rev. B 61 (2000) 6003–6018.
[30] H. Meher, Diffusion in intermetallics, Mater. Trans. JIM 37 (1996) 1259–1280.
[31] C.R. Kao, S. Kim, Y.A. Chang, Diffusional behavior in B2 intermetallic compounds, Mater. Sci. Eng. A 192/193 (1995) 965–974.
[32] G.P. Tiwari, R.S. Mehrotra, Kirkendall effect and mechanism of self-diffusion in B2 intermetallic compounds, Metall. Mater. Trans. A 43 (2012) 3654–3662.
[33] I.V. Belova, G.E. Murch, Interdiffusion in intermetallics, Metall. Mater. Trans. A 44 (2013) 4417–4421.
[34] N.A. Stolwijk, M. van Gend, H. Bakker, Self-diffusion in the intermetallic compound CoGa, Phil. Mag. A 42 (1980) 783–808.